Definition of Wind Loads on the Riyadh Western Metro Station

P. Schito(✉), L. Rosa, and A. Zasso

Department of Mechanical Engineering, Politecnico di Milano,
Via La Masa 1, 20156 Milan, Italy
{paolo.schito,lorenzo.rosa,alberto.zasso}@polimi.it

Abstract. Design of large modern structures can be strongly affected by wind actions, in terms of dynamic loading as well as peak façade cladding load. The wind forcing can be described by means of CFD analysis as well by wind tunnel tests using a scaled model instrumented with pressure taps. The density and the distribution of pressure taps on the building surface is critical, as well as the averaging of the surface pressure time history for the definition of the wind actions. Dynamic actions are calculated using a modal approach, while pressure excitation is computed according to time equivalent area averaging. The definition of the time equivalent area averaging is carefully analysed, in order to provide pressure values consistent with the forcing area.

Keywords: Wind loads · Wind tunnel tests · Dynamic response · TMD

1 Introduction

The design of modern large structures is often driven by the choice of architectural solutions that create emotion and wonder on the sightseers. The development of new construction technology by using more advanced materials, allows to designers to present structures with increasing complexity and innovative contents. Novel designs show complex shapes that sometimes cannot be reconducted to the building typologies reported in standard codes (i.e. Eurocode [1], ASCE [2]).

The design of current buildings uses several different materials for the different components of the building, up to the external surface, where the wind loads are transferred to the main structure. The size of the structure and its flexibility can be such that the wind pressure loads may induce deformations of the structure, leading to inertial accelerations that need to be considered in the structural design. Typically, in case of structures with very large dimensions, wind tunnel tests are required in order to consider the actual wind actions on the structure [3].

Wind tunnel tests on buildings are generally performed on rigid models, since, typically, the wind induced loads do not change significantly the shape of the building itself and its aerodynamic performances. Wind loads can be assessed by using an integral measurement (typically the forces on the building foundation) or by assessing the wind pressure acting on the building envelope. If both measurements are available, a verification of the reliability of the methodology can be conducted. Wind pressure is measured by means of pressure taps located on the building surface: the distribution of

F. Ricciardelli and A. M. Avossa (Eds.): INVENTO 2018, LNCE 27, pp. 679–688, 2019.
https://doi.org/10.1007/978-3-030-12815-9_51

the pressure taps must be suitable for the description of the wind action on the building. The calculation of the wind induced loads is generally performed taking into consideration the transient characteristics of the turbulent incoming wind with the dynamics of the structure.

Many strategies can be adopted for the calculation of wind loads on structures. CFD calculation can be used for the definition of the aerodynamic actions on the structure and the Standard recommended approach can be adopted to compute the wind loads, using the numerical model to extract the pressure coefficient distribution on the building surface. In this paper wind loads are extracted through wind tunnel tests using the high frequency pressure integration technique (HFPI), [4]. The practical basis of this approach is to develop an analytical modal approach considering as input the pressure data acquired simultaneously over the surface of the structure and the modal information (modal masses, mode shapes and frequencies) obtained from a finite element model of the structure. The calculation of the wind induced loads is generally performed taking into consideration the transient interaction of the turbulent incoming wind with the dynamics of the structure. The transient pressure distribution on the building surface is measured according to the incoming turbulent wind characteristics, that depend on the terrain characteristics and on the existing surrounding structures. The terrain features are estimated according to the area where the building will be erected (e.g. flat terrain – built environment) and indicates the main characteristics of the incoming wind in terms of vertical wind profile, vertical turbulence intensity and vertical turbulence length scale.

Fig. 1. Rendering of Riyadh Western Metro Station.

The structure that has been considered is the Riyadh Western Metro Station (see Fig. 1): it is a very light structure, mainly in steel, with length larger than 300 m and a height up to 25 m. The peculiar shape of the building and in particular of the smaller dune that acts as a cantilever produces very particular dynamic response of the structure.

2 Experimental Model

The wind tunnel model of Riyadh Western Metro Station has been realized with a geometrical scale of 1:100. Measurements were carried out for 36 wind directions spaced 10° apart, simulating the natural wind profile expected at the construction stage. Atmospheric boundary layer wind tunnel tests consider the characteristics of the natural wind, correctly scaled. In particular, the wind reproduces the variation of the mean velocity with the height from the ground and its turbulence characteristics. The simulation of the natural wind in the test section is achieved using passive turbulence generators placed at the beginning of the test section and roughness elements on the wind tunnel floor upstream the turntable (see Fig. 2). The model is designed to measure the pressures distribution by means of about 400 pressure taps simultaneously acquired. Pressure measurements are performed using the high-speed scanning pressure equipment Initium and the miniature pressure scanners ESP (*500* Hz sampling frequency). Pressure taps have been distributed on all surfaces of the dunes, including roof and façades (see Fig. 3). The model of the dunes was CNC made using resin. The external surface was left intentionally rough in order to simulate a higher Reynolds number and consequently a flow more similar to the full scale. The experimental setup considers not only the buildings, but also the most important surrounding buildings and the orography of the site.

Fig. 2. Wind tunnel model of Riyadh Western Metro Station.

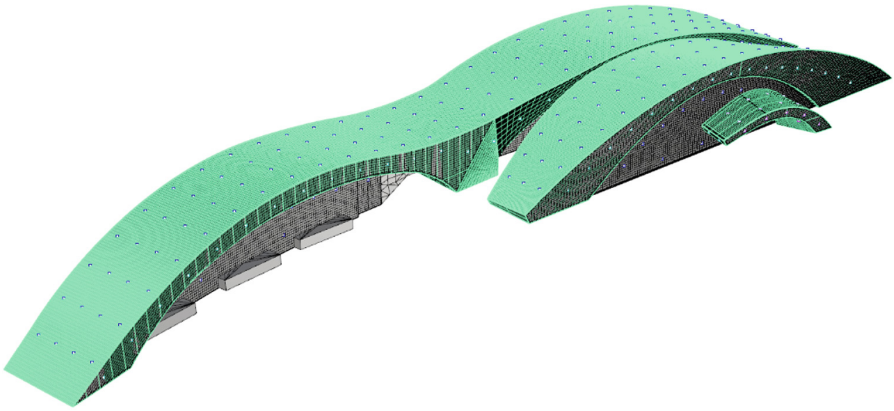

Fig. 3. Indication of pressure taps locations for the wind tunnel model.

3 Numerical Model

The computation of the wind loads is performed using the high frequency pressure integration technique (HFPI): the pressure data acquired simultaneously over the surface of the structure are coupled with the modal information (modal masses, mode shapes and frequencies) from a finite element model of the structure, to develop an analytical modal model of the building.

According to the modal approach, considering n modes, the vector of the nodal displacements $\boldsymbol{X}$ is expressed as:

$$\boldsymbol{X}(t) = \boldsymbol{\Phi}\underline{q}(t) \tag{1}$$

Where Φ is the matrix of the eigenvectors and $\underline{q}(t)$ is the vector of generalized displacements.

The equation of motion can be written as:

$$\boldsymbol{M}\ddot{\boldsymbol{X}}(t) + \boldsymbol{C}\dot{\boldsymbol{X}}(t) + \boldsymbol{K}\boldsymbol{X}(t) = \boldsymbol{F}(t) \tag{2}$$

$$\boldsymbol{\Phi}^{\boldsymbol{T}}\boldsymbol{M}\boldsymbol{\Phi}\underline{\ddot{q}}(t) + \boldsymbol{\Phi}^{\boldsymbol{T}}\boldsymbol{C}\boldsymbol{\Phi}\underline{\dot{q}}(t) + \boldsymbol{\Phi}^{\boldsymbol{T}}\boldsymbol{K}\boldsymbol{\Phi}\underline{q}(t) = \boldsymbol{\Phi}^{\boldsymbol{T}}\boldsymbol{F}(t) \tag{3}$$

$$\boldsymbol{M}_{\boldsymbol{q}}\underline{\ddot{q}}(t) + \boldsymbol{C}_{\boldsymbol{q}}\underline{\dot{q}}(t) + \boldsymbol{K}_{\boldsymbol{q}}\underline{q}(t) = \boldsymbol{Q}(t) \tag{4}$$

Where the forcing term $\boldsymbol{F(t)}$ is represented by the pressures acting on the cladding multiplied by its tributary area.

Displacements and accelerations are calculated by integrating, step by step, the equations of motion of the structure (Eq. 4).

Dynamic loads $\boldsymbol{F_{IN}}$ on each mass are calculated as:

$$\boldsymbol{F_{IN}}(t) = -\boldsymbol{m}\ddot{\boldsymbol{X}}(t) \tag{5}$$

The output of this analysis is the time history of the total loads (pressure loads on the cladding and inertial loads on the masses) on the entire structure. For the determination of the most critical situation, some strain indicators have been developed (e.g. maximum foundation moment).

The definition of the pressure loads is computed according to the instantaneous pressure measured on the experimental pressure taps, filtered according to the pressure tap reference area.

4 Spatial Averaging and the Aerodynamic Admittance Function

During wind tunnel tests, pressures are measured at specific points along the model. These punctual measurements are then used to compute the wind loads on finite areas. This passage, from pressure acting on a point to pressure acting on an area, needs a processing of the point pressure to account for the "spatial averaging" effect.

Indeed, fluctuating pressures acting on finite areas have smaller peak values than the pressure of a single point in that area. This occurs because, for a given area, the high frequency components of each punctual pressure are not fully correlated, and when these pressures are averaged over the finite area, the averaged fluctuations are smaller.

The "spatial averaging" effect is simulated by a "time filtering", using an appropriate filter function or "aerodynamic admittance" function, [5].

For standard structures, a moving average filter is generally used, with a time window equal to $\tau = KL/V$ being V the mean wind speed, L a characteristic length

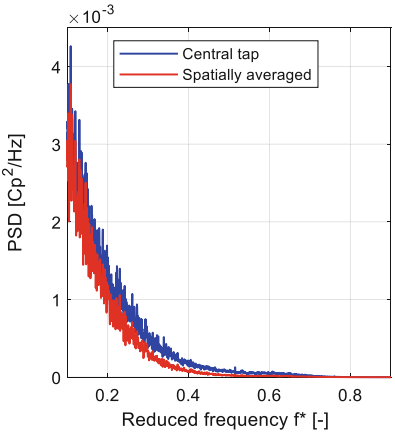

Fig. 4. PSD comparison between the central pressure tap in the tile and the spatially averaged signal, $\alpha = -135°$.

(e.g. diagonal of the tributary area), and K a number that depends on the structure (in general between 1−4, as described by Holmes [5]).

For complex structures like these dunes, specific tests should be performed to assess which is the effect of the "spatial averaging" and what is the appropriate processing of the time histories to simulate it. According to this method, the local pressure spectrum is multiplied by an "aerodynamic admittance" function that was experimentally evaluate. To evaluate the "aerodynamic admittance" the pressure was measured on a spatially dense array of pressure taps (hereafter called tile) in 3 significant finite areas of the surface (*20* taps for a *6* m^2 tile full scale), averaged, and finally compared with the single point measurement.

Signals acquired by the pressure taps in the tile were averaged at each time instant in order to obtain a new equivalent spatial averaged signal for each incoming wind direction. The new spatially averaged signal is assumed to be representative of the tile area.

As an example Fig. 4 shows the spectra of the time history of pressure acquired by the tap placed at the center of the tile and the spatially averaged signal for the same exposure angle. As one can see the spatially averaged signal has a lower energy content, especially for high reduced frequencies f^* ($f^* = f \cdot L/V$ where L is the diagonal of the tile and V is the design wind speed). It can be noted that for reduced frequencies higher than 0.5 the signals have no more energy content.

4.1 Experimental Admittance

Assuming that the spatial averaged signal is representative for the tile area, the transfer function (TF) between the signal of the tap placed at the center of the tile and the equivalent spatial averaged signal is computed for each exposure angle. This TF is called admittance function. Focusing on the most significant wind exposure angles in terms of dynamic contents, the transfer functions are plotted in Fig. 5, where the experimental TF (continuous line) is compared with the fitted curve (dashed line).

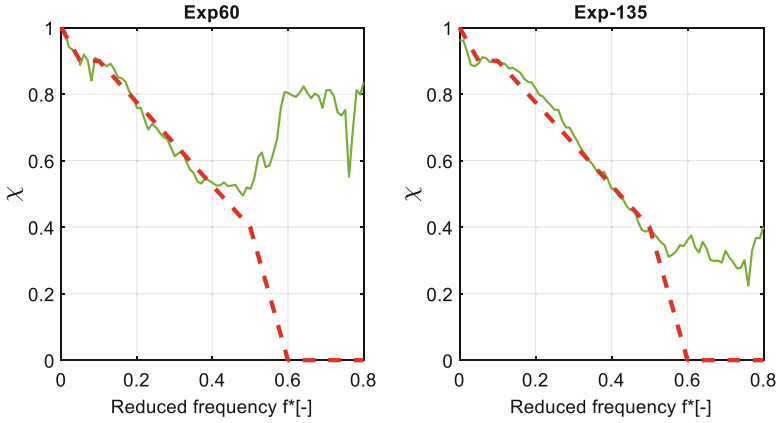

Fig. 5. Transfer Function module for wind exposure angles 60° and −135°.

TFs have been expressed as function of the reduced frequency f^*. It should be noted that for reduced frequencies higher than 0.5, the fitted curve approaches zero values, since we do not have energy content anymore (see Fig. 4) and thus it is no more significant since the signal contain only noise. The fitted aerodynamic admittance curve considers all the tiles and the wind directions, taking the most conservative case. The filter obtained with the previous procedure has been expressed as function of the reduced frequency. This makes possible to extend it to a generic surface of size L, with the hypothesis that the coherence between two points in an area it is not affected by the extent of the area, which is current practice.

5 Dune 0 Response to the Wind

The dynamic response of Dune 0 has been evaluated from the wind tunnel measured wind excitation. This is the most challenging structure since it is a standalone cantilevered structure almost *50* m long, see Fig. 6. Figure 7 shows the first and second vibrations mode of Dune 0, whereas in Fig. 8 the end section of Dune 0 is reported with its reference system.

The analysis considers a structural damping ratio of 0.7% and a mean incoming wind with return period of 100 years equal to V = 44 m/s. The numerical simulations were done for each exposure angles tested in the wind tunnel and the exposure angle $\alpha = 0°$ showed the worst dynamic response.

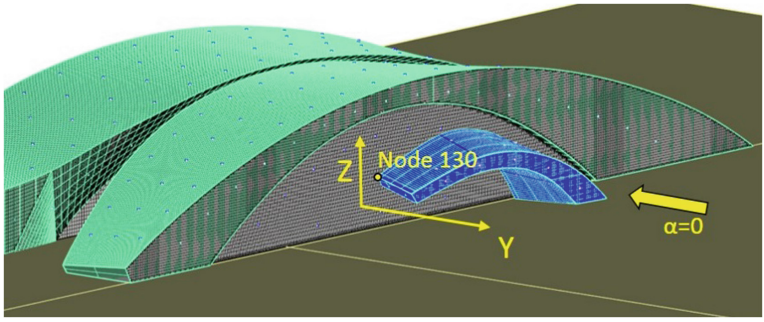

Fig. 6. Schematic model of Dune 0 and reference system.

The displacement of the dune 0 free end (monitoring the structural FEM node 130) shows large displacements and high accelerations along y-direction and z-direction, mainly imputable to the first mode shape of the structure. The displacement of node 130 showed values larger than ± 200 mm in the horizontal and vertical directions, while acceleration showed values that exceed *5* m/s^2. Figures 9 and 10 show the time histories of displacement and acceleration along y-direction (blue line), whereas the trend along z-direction (not shown here) was very similar. Figures 11 and 12 show the spectra of the previous time histories along y and z direction respectively (blue line): as one can see the contribution of the first vibration mode is prevalent and the intensity of the vibration along y and z directions is very similar.

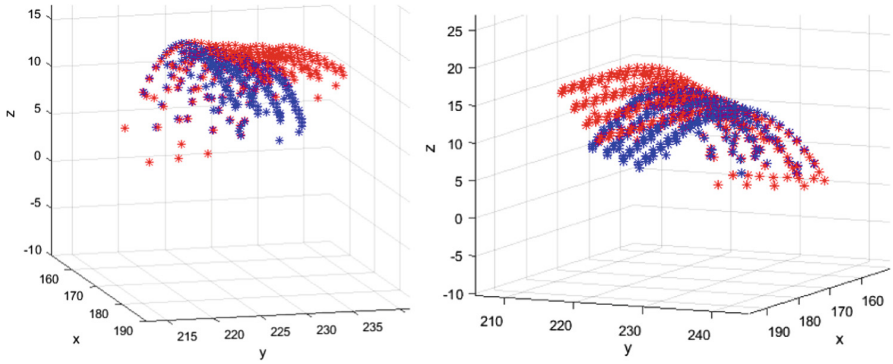

Fig. 7. First (sx) and second (dx) vibration mode of Dune 0. Blue points: not deformed geometry. Red points: mode shape.

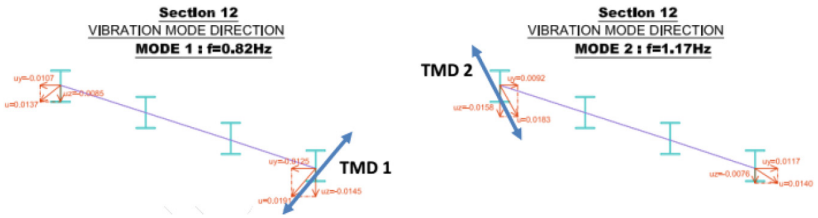

Fig. 8. Schematic model of the end section of Dune 0 and locations and direction of action for the installation of TMD.

The analysis of the data shows that both the displacements and accelerations evaluated were too high. Since it was not possible to modify the structure in order to increase its stiffness, it was necessary to increase the total damping of the structure by means of a tuned mass damper.

A preliminary study, by applying a damping ratio of *4%* on the first two modes, was conducted and the results are reported in Figs. 9 and 10 (red line). The displacements show values that exceed ± 75 mm, and accelerations slightly over *1.5* m/s^2. The signal spectrum (Figs. 11 and 12, red line) is largely reduced for the modes taken into account for the damping ratios of *4%*.

The reduction in oscillations and in accelerations seem satisfying with such damping ratio, therefore it was suggested to install two TMDs (each installed on the tip of the dune, and synchronized on its mode frequency). Each TMD should be working following the direction of the mode direction (following the maximum displacement value, that is located on the dune tip).

The modal mass of mode 1 was estimated in *30* tons, therefore a TMD with a weight of *0.6* tons is sufficient to guarantee the *4%* damping ratio. The modal mass of mode 2 is estimated in *50* tons, therefore a TMD with a weight of *1* ton is sufficient to guarantee the *4%* damping ratio. The location and direction of installation of TMDs is reported in Fig. 8.

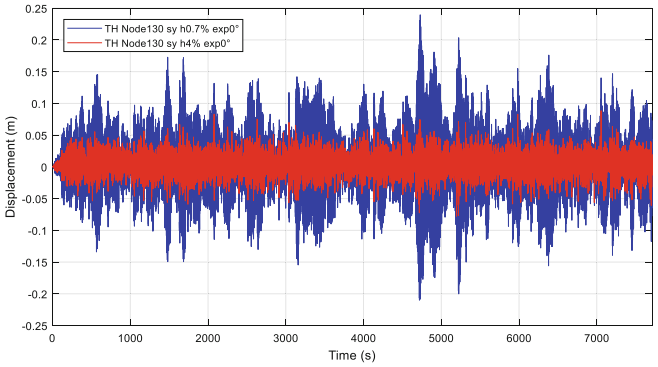

Fig. 9. Time history displacement FE node 130, y-direction, h = 0.7% and h = 4%.

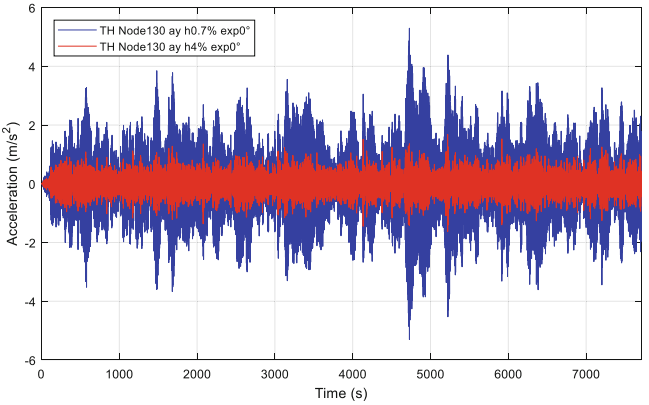

Fig. 10. Time history acceleration FE node 130, y-direction, h = 0.7% and h = 4%.

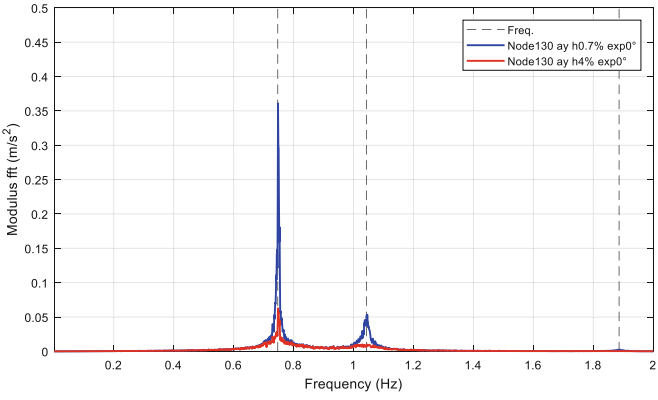

Fig. 11. Spectra acceleration FE node 130, y-direction, h = 0.7% and h = 4%.

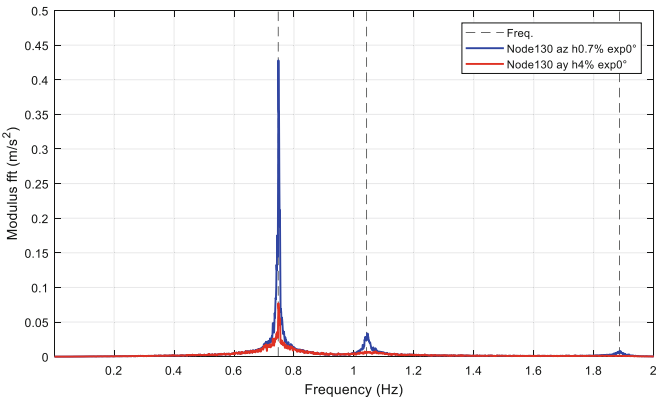

Fig. 12. Spectra acceleration FE node 130, z-direction, h = 0.7% and h = 4%.

As an alternative option, it would be possible to have each damper vertically guided, by increasing, roughly proportionally, the overall damping masses.

6 Conclusions

The method described in this article shows how it is possible to combine a modal approach analysis, with experimental wind tunnel test in order to simulate the dynamic of a structure. Results achieved with a rigid model are used to load a numerical model of the structure in order to evaluate the dynamic response of the structure. The wind excitation is extrapolated from measured wind tunnel data, by deriving the loading on the cladding surface of the structure, by taking into consideration the extension of the area and the equivalent loading, through an admittance function. The response of the building is evaluated and, by applying an equivalent damping to the structure, the displacements and the accelerations of the structures are limited. The required damping system, using a TMD technology is evaluated, and an estimation of the requirements of the system are presented.

References

1. Eurocode1 (2005) UNI EN 1991-1-4. Actions on structures - Part 1-4: General actions - Wind actions, April 2005
2. ASCE 7-05. Minimum Design Loads for Buildings and Other Structures
3. Irwin PA (2009) Wind engineering challenges of the new generation of super-tall buildings. J Wind Eng Ind Aerodyn 97(7–8):328–334
4. Rosa L, Tomasini G et al (2012) Wind-induced dynamics and loads in a prismatic slender building: a modal approach based on unsteady pressure measurements. J Wind Eng Ind Aerodyn 107–108:118–130
5. Holmes JD (1997) Equivalent time averaging in wind engineering. J Wind Eng Ind Aerodyn 72:411–419